Eur. Phys. J. B **21**, 437–445 (2001)

THE EUROPEAN PHYSICAL JOURNAL B

EDP Sciences

Surface shear horizontal waves associated with a periodic array of wires deposited on a substrate

A. Khelif[1,a], B. Djafari-Rouhani[2], and Ph. Lambin[1]

[1] Laboratoire de Physique du Solide, Département de Physique, Facultés Notre-Dame de la Paix, 5000 Namur, Belgium
[2] Laboratoire de Dynamique et Structure des Matéraiux Moléculaires, UPRESA CNRS 8024, Université des Sciences et Technologies de Lille, 59655 Villeneuve d'Ascq, France

Received 6 December 2000

Abstract. The vibrational and electronic spectra of a semi-infinite crystal with a planar surface are modified by the presence of surface inhomogeneities or roughness such as ridges or grooves, quantum wires or tips. We develop a Green's function formalism to investigate the localized and resonant acoustic modes of shear horizontal polarization associated with the surface of a substrate supporting a single and a periodic array of wires. Each material is assumed to be an isotropic elastic medium. The calculation can be applied to an arbitrary choice of the shape and elastic parameters of the wires. The surface modes are obtained as well-defined peaks of the densities of states (DOS). In this paper, we calculate the variation of the density of states associated with the adsorption of a single wire, and the dispersion curves of the surface modes for a periodic array of wires on the flat surface of a substrate. We discuss their behaviors as a function of the elastic parameters and the relationship between resonant modes of the single wire and dispersion curves of the surface modes for a periodic structure.

PACS. 43.40.+s Structural acoustics and vibration – 43.20.+g General linear acoustics – 62.30.+d Mechanical and elastic waves; vibrations

1 Introduction

With the progress of techniques such as microlithography or molecular beam epitaxy, it is possible to create well defined micro- or nanostructures on an otherwise planar surface. These surface defects modify the physical properties of the crystal surface that in turn can serve as a tool for the characterization of the surface inhomogeneities. Several works have been devoted to the study of surface acoustic vibrations in presence of a single [1–4] or periodic [5–16] array of resonating elements. In particular, the periodically corrugated surface of an elastically isotropic substrate can support localized shear horizontal modes, in contrast to the case of a substrate with a flat surface. The propagation of surface acoustic waves across a grating or a periodic array of wires deposited on a substrate is of great current interest for several reasons: the system is a model for randomly rough surfaces that can be studied exactly and the results obtained in this work help to interpret the observations for randomly rough surfaces. In the system such as investigated here, there can be a conversion of surface acoustic waves into bulk waves and the result of our calculations could well be useful in the design of filters for surface acoustic waves and transducers.

The aim of this paper is to investigate both localized and resonant acoustic modes of shear horizontal polarization associated with the surface of a substrate supporting a single wire and a periodic array of wires. We have developed an exact numerical method by using a Green's function formalism to obtain the local densities of states (DOS) at every point inside the substrate and inside the wires. With this method we deduce the dispersion curves from well-defined peaks of the DOS for a periodic array wires. The calculation can be performed for an arbitrary choice of the shape and elastic parameters of the wires. The method has been previously applied to the study of acoustic shape resonances of a single wire [3,4] as well as to investigate the scattering properties of an incident plane wave by such a wire [17]. The main novelty in this work lies in the calculation of the DOS, and accordingly the dispersion curves of both localized and resonant modes, for a periodic array of wires, with an arbitrary choice of their composition and geometry [16]. The dispersion curves are presented as a function of the wavevector k parallel to the surface and perpendicular to the wires, k being limited to the first Brillouin zone, namely $-\pi/P < k < \pi/P$ where P is the period. The localized modes lie below the bottom of the substrate bulk band, while the resonances fall in the radiative zone inside this band. We also discuss the behavior of the dispersion curves as a function of

[a] e-mail: abdelkrim.khelif@fundp.ac.be

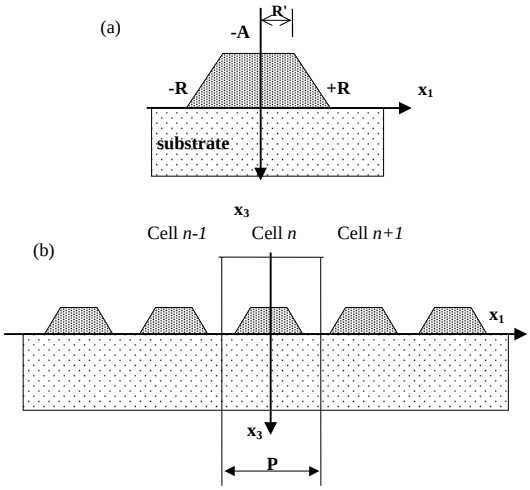

Fig. 1. Schematic of the geometry investigated in this work: a single wire (a), or a periodic array of wires (b) adsorbed on a substrate.

the material parameters (elastic constants and mass densities), in particular their interaction with the sound line of the substrate folded back into the first Brillouin zone. At the end, we compare the frequency positions of these branches with the resonant modes of individual wires.

Section 2 contains a brief presentation of the theoretical formalism. Section 3 is devoted to the discussion of the DOS and the dispersion curves. The conclusions are drawn in Section 4.

2 Theoretical formalism

The geometry of the supported wires is sketched in Figure 1. The wires are oriented parallel to the x_2-axis, perpendicular to the drawing plane.

We assume that the wires are fabricated from a material of mass density $\rho^{(a)}$ and elastic modulus $C_{44}^{(a)}$. They are bonded to a semi-infinite substrate fabricated from a material of a mass density $\rho^{(b)}$ and elastic modulus $C_{44}^{(b)}$. Each material is assumed to be an isotropic and homogeneous elastic medium.

The substrate fills the region $x_3 > 0$ of the space. In these structures the displacement field of the shear horizontal vibration has a single component parallel to the axis of the wires and can be written as:

$$u(x,t) = [0, u_2(x_1, x_3|\omega), 0] \exp(-\mathrm{i}\omega t), \tag{1}$$

where ω is the frequency of the wave. The equation of motion satisfied by the component $u_2(x_1, x_3|\omega)$ in each medium is:

$$C_{44}^{(i)} \left(\frac{\partial^2}{\partial x_1^2} + \frac{\partial^2}{\partial x_3^2} + \frac{\omega^2}{C_t^{(i)2}} \right) u_2(x_1, x_3|\omega) = 0, \tag{2}$$

and is subject to the usual boundary conditions, namely vanishing normal stress at the free surface and continuity of the displacement and the normal stress at the substrate-wire interface. In equation (2), $C_t^{(i)}$ is the transverse velocity of sound in medium "i" defined by

$$C_t^{(i)} = \sqrt{\frac{C_{44}^{(i)}}{\rho^{(i)}}} \cdot \tag{3}$$

The Green's function of the system is also given by an equation similar to equation (2), *i.e.*

$$C_{44}^{(i)} \left(\frac{\partial^2}{\partial x_1^2} + \frac{\partial^2}{\partial x_3^2} + \frac{\omega^2}{C_t^{(i)2}} \right) G_i(x_1, x_3; x_1', x_3'|\omega) = \delta(x_1 - x_1')\delta(x_3 - x_3'), \tag{4}$$

together with the appropriate boundary conditions.

In the case of an infinite homogeneous solid or of a semi-infinite substrate with a planar free surface, the solution of equation (4) is known analytically and can be expressed with the help of the Hankel function of the first kind as [18]

$$G_i(x_1, x_3; x_1', x_3'|\omega) = \frac{-\mathrm{i}}{4C_{44}^{(i)}} H_0^{(1)} \left(\frac{\omega}{C_t^{(i)}} \left[(x_1 - x_1')^2 + (x_3 - x_3')^2 \right]^{1/2} \right), \tag{5}$$

for the bulk and

$$g_i(x_1, x_3; x_1', x_3'|\omega) = \frac{-\mathrm{i}}{4C_{44}^{(i)}} \times \left[H_0^{(1)} \left(\frac{\omega}{C_t^{(i)}} \left[(x_1 - x_1')^2 + (x_3 - x_3')^2 \right]^{1/2} \right) + H_0^{(1)} \left(\frac{\omega}{C_t^{(i)}} \left[(x_1 - x_1')^2 + (x_3 - x_3')^2 \right]^{1/2} \right) \right], \tag{6}$$

for the semi-infinite medium.

From the knowledge of G_i and g_i, one can calculate the matrix elements of the Green's function in the final composite systems. We use the formalism of the interface response theory [3,19] in which the calculation is first performed in the reduced space of interfaces before being extended to the whole material. In the following, we shall call M_1 and M_2 the parts of the surface of a wire which are respectively in contact with vacuum and with the substrate, and define $M = M_1 \cup M_2$ as being the space of interfaces. The creation of both geometries in Figure 1, can be accomplished schematically through the following two operations.

2.1 Creating an isolated wire

First, an isolated wire is extracted from an infinite material "a" by the application of a cleavage operator V_a which cuts the finite object out of the infinite solid

$$V_a(x_1, x_3) = C_{44}^{(a)} \frac{\partial}{\partial n}, \tag{7}$$

$$\exp\left(\mathrm{i}\left[\frac{\omega}{C_t}(X_1-X_1')-\frac{\pi}{4}\right]\right)\left(A_1\left[\frac{X_1-X_1'}{P}\right]+A_2\left[\frac{X_1-X_1'}{P}\right]^2+A_3\left[\frac{X_1-X_1'}{P}\right]^3+A_4\left[\frac{X_1-X_1'}{P}\right]^4\right)$$
$$+\exp\left(-\mathrm{i}\left[\frac{\omega}{C_t}(X_1-X_1')+\frac{\pi}{4}\right]\right)\left(B_1\left[\frac{X_1-X_1'}{P}\right]+B_2\left[\frac{X_1-X_1'}{P}\right]^2+B_3\left[\frac{X_1-X_1'}{P}\right]^3+B_4\left[\frac{X_1-X_1'}{P}\right]^4\right), \quad (15)$$

where $\frac{\partial}{\partial n}$ means the normal derivative at the point (x_1, x_3) of the boundaries.

The Green's function g_a of the finite wire in the interface space M of this wire satisfies an integral equation which can formally be written as [3,19,20]:

$$g_a(M,M)[I(M,M)+V_a(M,M)G_a(M,M)] = G_a(M,M), \quad (8)$$

where I is the identity matrix.

2.2 Coupling the wires to the substrate

Let us distinguish the case of a single wire from the case of the periodic array of wires.

2.2.1 Single wire

The isolated wire "a" is coupled to the substrate "b" through its interface M_2. Because we are dealing with continuous media, we obtain the following form for the Green's function g_f of the final system in the interface space M_2 [18,19]

$$g_\mathrm{f}^{-1}(M_2M_2) = g_a^{-1}(M_2M_2) + g_b^{-1}(M_2M_2), \quad (9)$$

where $g_a(M_2M_2)$ is a truncated matrix obtained from $g_a(MM)$.

Both equations (8) and (9) are integral equations which, for the numerical resolution, are converted into discrete equations [3,4,17], taking careful account of the singular behavior of the Green's function and their derivatives in the limit $x \to x'$.

2.2.2 Periodic wires

The wires are coupled to the substrate through their interfaces $M_2^{(n)}$, where the superscript n refers to the numbering of the wires. Defining $\overline{M} \cup_n M_2^{(n)}$, one obtains:

$$g_\mathrm{f}^{-1}(\overline{M},\overline{M}) = g_b^{-1}(\overline{M},\overline{M}) + g_a^{-1}(\overline{M},\overline{M}). \quad (10)$$

Owing to the absence of interaction between the wires before their coupling to the substrate, this equations can also be written as:

$$g_\mathrm{f}^{-1}(\overline{M},\overline{M}) = g_b^{-1}(\overline{M},\overline{M}) + \sum_n g_a^{-1}(M_2^{(n)},M_2^{(n)}). \quad (11)$$

On the other hand, one can take advantage of the periodicity along the direction x_1 to perform a Fourier transform and express equation (10) in only one unit cell for every value of the wavevector k parallel to x_1 which is limited to the first Brillouin zone, *i.e.*, $-\pi/P < k < \pi/P$. Then, equation (11) can be written in a mixed (real space-reciprocal space) representation as

$$g_\mathrm{f}^{-1}(X_1,X_1'|k\omega) = g_a^{-1}(X_1,X_1') + g_b^{-1}(X_1,X_1'|k\omega), \quad (12)$$

where the real space part (X_1) can be limited to one single unit cell, let us say $M_2^{(0)}$. To calculate the inverse of the substrate Green's function in the mixed representation $g_b^{-1}(X_1,X_1'|k\omega)$, it is first necessary to Fourier transform $g_b(x_1,x_1'|\omega)$. In that way we have from equation (6) for $x_3 = 0$:

$$g_b(X_1,x_3=0;X_1',x_3'=0|k\omega) = \sum_{n=-\infty}^{+\infty}\frac{-\mathrm{i}}{2C_{44}^{(b)}}H_0^{(1)}\left[\frac{\omega}{C_t^{(b)}}(|X_1-X_1'+nP|)\right]\exp(\mathrm{i}knP). \quad (13)$$

We propose the following original method to calculate the above series. The first few terms of the Fourier series (up to $n_0 = 50$) are computed exactly, while the next terms are evaluated by using the following asymptotic behavior of the Hankel function for large arguments:

$$H_0^{(1)}(z) \cong \sqrt{\frac{2}{\pi z}}[f(z)+\mathrm{i}Q(z)]\exp\left(\mathrm{i}\left(z-\frac{\pi}{4}\right)\right), \quad (14)$$

where $f(z) = 1 - \frac{9}{128z^2} + \frac{11\,025}{9\,830z^4} + \ldots$, and $Q(z) = -\frac{1}{8z} + \frac{225}{3\,072z^3} + \ldots$ By injecting the asymptotic behavior equation (14) in equation (13) and making a Taylor expansion with respect to the small quantity $\frac{|X_1-X_1'|}{nP}$, the asymptotic terms of equation (13) can be cast into the form:

see equation (15) above,

where A_n and B_n are coefficients that depend on frequency and wave vector. Their expressions are given in the Appendix.

The advantage of the above method relies on the fact that the coefficients A_n and B_n are calculated for each frequency ω and wavevector k, but independently of the spatial position X_1 or X_1'. Therefore, it is much faster to calculate the expression (15) for every value of $(X_1 - X_1')$ than evaluating the expression (13) that contains explicitly the Hankel function.

Once the elements of the Green's function in the interface space are known in the two geometries (single and periodic wires), all the matrix elements can be obtained through the equation [19]:

$$g_{\rm f}(DD) = g_{\rm r}(DD) + g_{\rm r}(D,M) \times [g_{\rm r}^{-1}(MM)g_{\rm f}(MM) - I(MM)]g_{\rm r}^{-1}(MM)g_{\rm r}(MD), \quad (16)$$

where D is the whole space of the material and $g_{\rm r}$ the Green's function of the reference system composed of uncoupled substrate and wires. The knowledge of $g_{\rm f}$ in the space D enables us to calculate the local density of states at any point inside the wires or the substrate

$$n(x,\omega) = \frac{-2\omega}{\pi}\rho(x){\rm Im}\, g_{\rm f}(x,x). \quad (17)$$

It should be noted that for a periodic geometry (Fig. 1b) one has to substitute $x \to (X_1, x_3)$ where X_1 is limited to only one unit cell.

3 Discussion of the densities of states and dispersion curves

In this section we present and comment on a few calculations of the local and total density of states and dispersion curves for localized and resonant modes. In these calculations we assume that the wires have a trapezoidal shape (see Fig. 1), this means they are bounded by the following equation

$$\zeta(x_1) = \begin{cases} -A & \text{for} \quad |X_1| \le R' \\ A\dfrac{(X_1 - R)}{R - R'} & \text{for} \quad R' < |X_1| < R, \end{cases} \quad (18)$$

and in most of the following illustrative examples we have taken $A = 2R$ and $R'/R = 1/4$. In the discretization of integral equations, the interval $[-R, R]$ is divided into $2N$ equal parts, with $N = 100$.

3.1 Single wires

Owing to the symmetry of the geometry, the acoustic resonances may be distinguished according to their symmetric or antisymmetric character.

Figure 2 gives the variation $\Delta n(\omega) = n_{\rm f}(\omega) - n_b(\omega)$ of the total density of states due to the deposition of the wire onto the planar surface. For comparison, we have also displayed in each panel the local densities of states integrated either along the planar interface between the wire and the substrate or along the free surface of the wire. In these few examples the two materials may either be identical or have different mass densities and elastic constants. When the wire is deposited on a substrate, the acoustic resonances appear as well-defined peaks of the total and local DOS (see Fig. 2). In panels (a) (symmetric modes) and (b) (antisymmetric modes) these DOS are calculated in the case of a wire made of the same material as the substrate, which can be considered as a model of surface roughness. There is a connection between the peaks of the density of states and the discrete eigenfrequencies of an isolated (not supported) wire with stress-free surface. This correspondence becomes more pronounced by stiffening the material of the wire, *i.e.* by taking $C_{44}^{(a)} \gg C_{44}^{(b)}$ (panels (c) and (d)). This behavior can be understood on the basis of the continuity of the normal stress at the substrate-wire interface, namely the wire behaves like an unsupported medium when its elastic constant becomes much larger than that of the substrate. In the same way, when the wire is softer than the substrate, *i.e.* $C_{44}^{(b)} \gg C_{44}^{(a)}$ (panels (e) and (f)), we can establish a connection between the peaks in the DOS and the eigenfrequencies of an isolated wire that has its boundary (M_2) with the substrate rigidly fixed, the boundary with vacuum (M_1) being still free of stress (we refer to such a situation as mixed boundary conditions [3,4]).

The lowest two panels in Figure 2 give the DOS when the substrate and the wire have the same elastic constant but differ by their mass densities. When the substrate is much denser than the wire, *i.e.* $\rho^{(b)} \gg \rho^{(a)}$ (panels (g, h)), the peaks in the total DOS occur approximately at the same frequencies as those obtained for a hard substrate (panels (e, f)). On the other hand, for a light substrate $\rho^{(a)} \gg \rho^{(b)}$ (panels (i, j)), one can only notice an approximate similarity with the results of panels (c, d) corresponding to a soft substrate, with however a slight shift for the low frequency symmetric resonance that may originate from the static ($\omega = 0$) mode of the isolated wire.

Another point to notice in all the above illustrations concerns the similarity between the peaks in the total DOS and those in the average local DOS at the free surface (M_1) of the wires. In contrast, the peaks in the local DOS at the substrate-wire interface (M_2) may happen at the same frequencies as those of the total DOS (panels (a, b), (c, d) or (i, j)), or be shifted with respect to the latter (panels (e, f) or (g, h)). Indeed, unlike the interface, the boundary condition at the free surface (M_1) is not sensitive to the relative change of the elastic parameters.

These peaks in the density of states for a single wire will help us in understanding the dispersion curves of a periodic structure.

3.2 Periodic wires

In this section, we present a few illustrations of the DOS and resulting dispersion curves for the localized and resonant modes.

First, we assume that the substrate is made of a material with a higher elastic constant than the wires, and the geometrical parameters are taken to be: $A/R = 2$, $P/R = 2.1$ and $R'/R = 1/4$. Figure 3 gives an example of the average local density of states at the free surface of each wire. Remember that the behavior of the total DOS resembles that of the local DOS at the free surface.

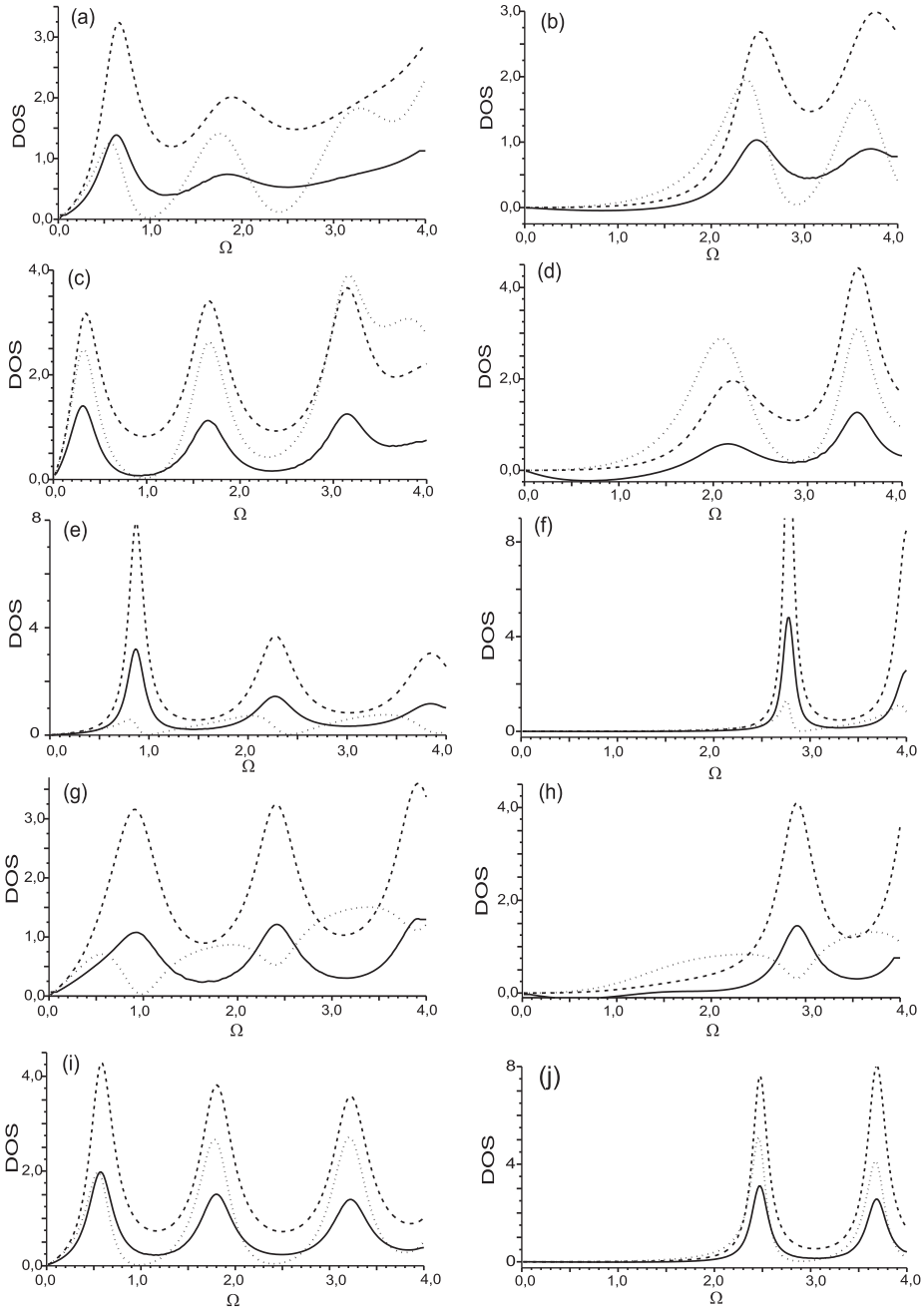

Fig. 2. Resonant modes associated with an adsorbed wire "*a*" on the substrate "*b*". The full lines give the variation in the total density of states (in units of $R/C_t^{(a)}$) as a function of $\Omega = \omega R/C_t^{(a)}$; with $2R$ the long basis of the trapezoidal wire. The dashed and dotted lines respectively give the local density of states (in units of $(4C_t)^{-1}$) integrated along the free surface and along the substrate-wire interface. Left (resp. right) panels correspond to the symmetric (resp. antisymmetric) modes. The elastic parameters are defined as: panels (a) and (b) $C_{44}^{(a)}/C_{44}^{(b)} = 1$, $\rho^{(a)}/\rho^{(b)} = 1$; (c) and (d) $C_{44}^{(a)}/C_{44}^{(b)} = 4$, $\rho^{(a)}/\rho^{(b)} = 1$; (e) and (f) $C_{44}^{(a)}/C_{44}^{(b)} = 0.25$, $\rho^{(a)}/\rho^{(b)} = 1$; (g) and (h) $C_{44}^{(a)}/C_{44}^{(b)} = 1$, $\rho^{(a)}/\rho^{(b)} = 0.25$; (i) and (j) $C_{44}^{(a)}/C_{44}^{(b)} = 1$, $\rho^{(a)}/\rho^{(b)} = 4$.

In this figure, the DOS are sketched for several values of the wavevector k ranging from 0 to π/P. At the lowest wavevector (Fig. 3a), one can notice a very sharp and narrow peak that appears below the bottom of the substrate bulk band defined by the sound line $\omega = C_t^{(b)}\, k$ (marked by an arrow under the frequency axis). This peak is associated with a surface localized mode. By increasing the wavevector k (Figs. 3b, c, d), a second and a third surface mode also emerges from the bulk band. Besides the localized modes, there are also several well-defined peaks of the DOS existing inside the bulk band of the substrate that are associated with resonant (or leaky) waves. The shape and intensities of these peaks significantly depend upon the wavevector k; however, their frequencies are

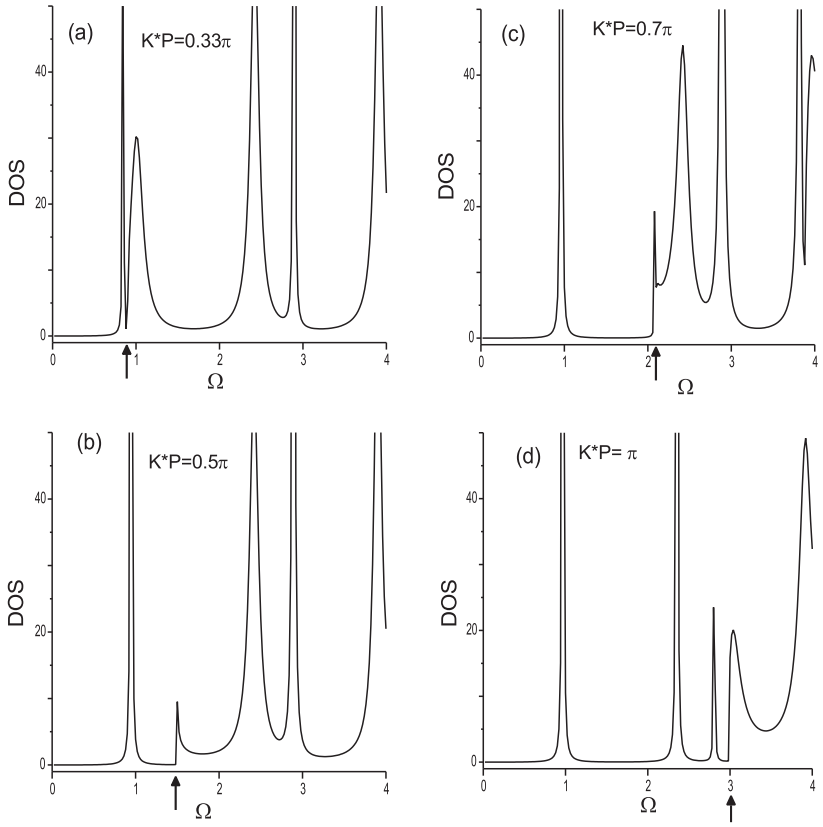

Fig. 3. Average local density of states at the free surface of each wire for four different values of the wavevector k. The dimensionless frequency is defined as $\Omega = \omega R/C_t^{(a)}$. The parameters are the following $C_{44}^{(a)}/C_{44}^{(b)} = 0.25$, $\rho^{(a)}/\rho^{(b)} = 1$, $A = 2R$, $R'/R = 1/4$, $P/R = 2.1$. The arrow under the frequency axis indicates the bottom of the bulk band.

almost independent of k except in the vicinity of the points where their dispersion curves cross the sound line folded back into the first Brillouin zone (see also Figs. 4–6 below).

From the calculations of the DOS, one can obtain a general view of the dispersion curves of the localized and resonant modes as a function of the different parameters involved in the problem, namely the period P, the shape (or geometry) of the wires and the material parameters (*i.e.* the contrast between the elastic constants and mass densities of the wires and the substrate). The results are illustrated in Figures 4–6 where we represent a series of gray-scale DOS maps as a function of the frequency ω and the wavevector k. The advantage of this presentation is to illustrate both the dispersion curves and the widths (or lifetimes) of the resonant states.

First, we discuss in Figure 4 the behavior of surface modes as a function of the period P by plotting the dispersion curves for $P/R = 2.1$ (Fig. 4a) and $P/R = 3$ (Fig. 4b). We assume here that the wires and the substrate are made of the same material, and the geometrical parameters are $A/R = 2$ and $R'/R = 1/4$. In both panels, there is one surface branch below the bulk band, that is associated with a localized mode. However, as we shall see in the next figures, the number of localized modes may be increased or decreased by changing the geometrical and/or the elastic parameters. In the long wavelength limit (small wavevector k) the surface branch is tangent to the sound line $\omega = C_t^{(b)}\, k$. At higher wavevectors, the dispersion curve bends away from the sound line and displays the phenomenon of wave slowing, *i.e.* slowing down of the phase and group velocities. Also, the localization of the surface mode increases near the Brillouin zone edge because the surface branch becomes more separated from the bulk band. These effects are more important in the case $P/R = 2.1$ where the distance between the wires is smaller.

Besides the localized modes, the Green's function method also enables us to obtain the dispersion curves of the resonant states which fall inside the bulk band. One can notice that these curves are in general rather flat and widened. However, they display a bending when they cross the sound line folded back into the first Brillouin zone. The narrow frequency domains covered by these resonances coincide well with the corresponding resonances of a single supported wire. Indeed, the lowest discrete modes of the single wires give rise to the surface localized branches, whereas the highest modes fall inside the substrate bulk band and become resonant branches.

Figures 5 illustrate the dependence of the dispersion curves with the geometrical parameters of the wires, namely the height A and the ratio R'/R of the bases of the trapeze in Figure 1. In Figure 5a, where the dispersion curves are given for $A/R = 4$, one can notice an increase in the number of surface modes as compared to Figure 4a

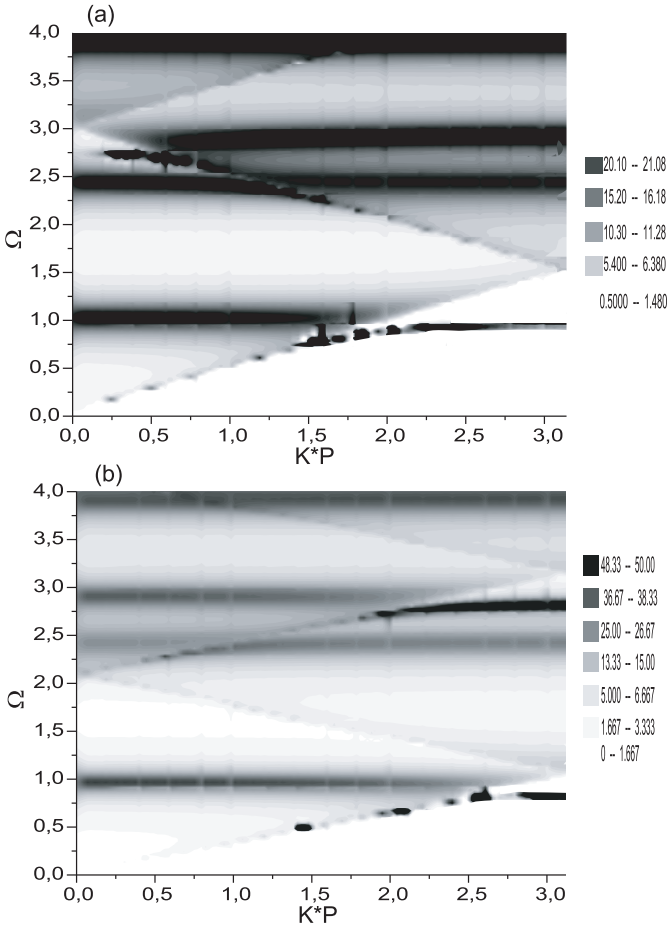

Fig. 4. Dispersion curves of the localized and resonant modes as a function of the reduced wavevector kP for two different periods: (a) for $P/R = 2.1$ and (b) $P/R = 3$. The wires are assumed to be made of the same material as the substrate, the geometrical parameters are $A = 2R$ and $R'/R = 1/4$.

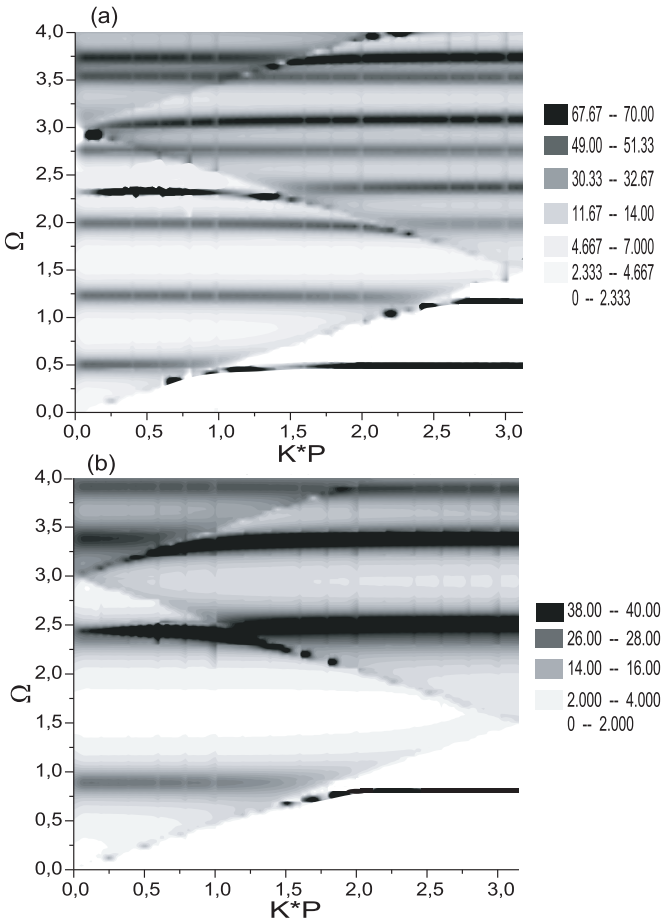

Fig. 5. Same as in Figure 4a, except that in panel 5a $A = 4R$ and in panel 5b $R'/R = 1/2$.

where $A/R = 2$. This behavior is related to the increase in the size of the wires and is in agreement with the results obtained in previous works for the localized modes of a rectangular [9] or sinusoidal [14] grating ruled on the surface of a substrate. In particular, there are two branches of localized modes below the substrate bulk band and several resonant branches in the frequency domain displayed in Figure 5a.

In Figure 5b we have changed the other geometrical parameter of the model, namely the ratio R'/R is taken to be $1/2$ instead of $1/4$ as in Figure 4a. This has the effect of bending more strongly the localized branch, and also induces some modifications of the DOS inside the bulk band.

Finally, in Figure 6, we illustrate the behavior of the dispersion curves for different elastic parameters of the wires as compared to those of the substrate. Regarding the localized surface branches, one can distinguish two typical behaviors depending on the ratio $c = \frac{C_t^{(a)}}{C_t^{(b)}}$ between the sound velocities in the wires and in the substrate. In the first situation $c < 1$ – which can be realized by assuming that the substrate has a higher elastic constant (Fig. 6a) or a lower mass density (Fig. 6b) than the wires – the surface branch more strongly bends near the Brillouin zone edge, and even higher surface branches can emerge from the bulk band. In contrast, in the opposite situation $c > 1$ – which can be obtained if the substrate has a lower elastic constant (Fig. 6c) or a higher mass density (Fig. 6d) than the wires – the surface branch lies very close to the bulk band and may even disappear by changing the geometrical parameters of the wires or the period of the array (for instance by decreasing the ratio R/P, *i.e.* by increasing the period as compared to the size of the wires). One can point out a more important localization of the surface waves in the case $c < 1$ than in the opposite situation. Figure 6 also contains the dispersion curves of the resonant modes. As mentioned before, these branches remain, in general, rather flat and their frequencies are in close agreement with those of the resonant modes of a single wire; however, one can notice an interaction of these modes with the sound line folded back into the first Brillouin zone which gives rise to a bending of the dispersion curves around these crossing points.

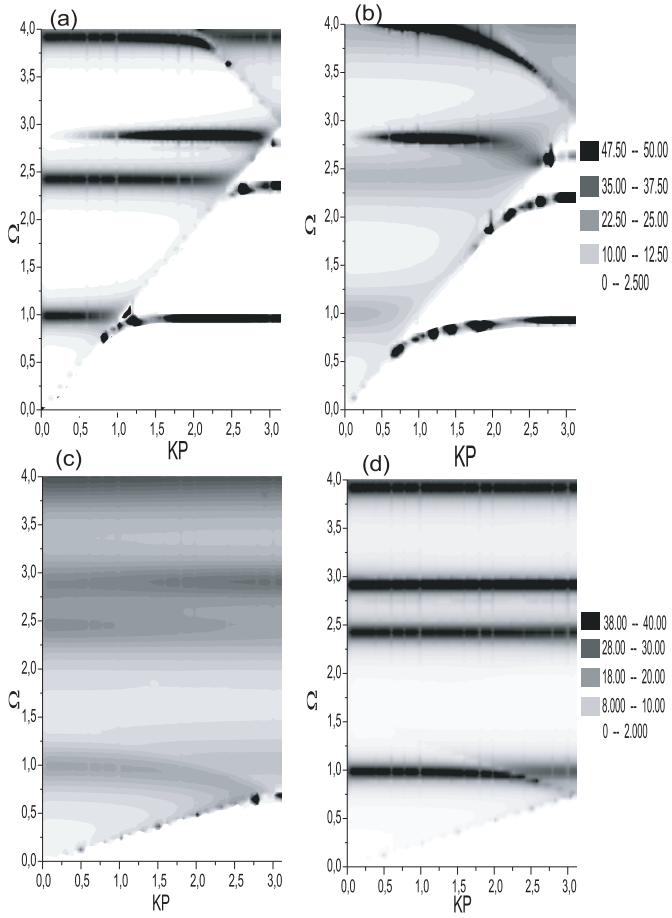

Fig. 6. Same as in Figure 4a but for different elastic parameters of the wires and the substrate: (a) $C_{44}^{(a)}/C_{44}^{(b)} = 0.25$, $\rho^{(a)}/\rho^{(b)} = 1$; (b) $C_{44}^{(a)}/C_{44}^{(b)} = 1$, $\rho^{(a)}/\rho^{(b)} = 4$; (c) $C_{44}^{(a)}/C_{44}^{(b)} = 4$, $\rho^{(a)}/\rho^{(b)} = 1$; (d) $C_{44}^{(a)}/C_{44}^{(b)} = 1$, $\rho^{(a)}/\rho^{(b)} = 0.25$.

4 Conclusion

The main object of this paper was to develop a new theoretical method to investigate the vibrational properties of a single ridge and, more especially, of a periodic array of ridges deposited on a substrate. The interest of the method relies on its capability of treating any geometry and composition (elastic parameters) of the wires. The calculation is based on a Green's function formalism in which the local DOS can be obtained at every point inside the wires or inside the substrate. From the knowledge of these quantities, we have studied the surface localized and resonant modes associated with the wires for various physical and geometrical parameters of the system. Lets us notice that an extension of this work [17] can also enable us to obtain the scattering of an incoming acoustic wave from the corrugated surface and, therefore, may have applications in the topic of near field microscopy or nondestructive testing.

The above method was first applied to obtain the acoustic shape resonances of a single ridge. Both the contrasts between the elastic constants and between the mass densities are important for the determination of the resonance frequencies. The linewidths of the peaks are related to the lifetimes of these excitations. In some limiting cases of a very soft or of a very hard wire, the resonance frequencies become comparable to those of an isolated (non supported) wire with appropriate boundary conditions.

The second application of the method was dealing with a periodic array of wires. The number and dispersion of the localized branches (situated below the substrate sound line) are very dependent upon the geometrical and elastic parameters of the wires. Qualitatively, this number increases (resp. decreases) either by softening (resp. hardening) the wires as compared to the substrate or by increasing (resp. decreasing) the height of the wires. These general trends are of course very similar to those of the Love modes associated with an adlayer deposited on a substrate. Roughly speaking, our system of periodic wires separated from each other by vacuum can be considered as an effective coating adlayer, with however a lower mass density and a lower elastic constant than in the actual wires. This is particularly true in the long wavelength limit. Nevertheless, when the wavelength decreases, the true system differs from the coated substrate by the existence of the Brillouin zone associated with the periodicity of the wires. As a consequence, there is a bending of the dispersion curves near the zone boundary that leads to a slowing down of the phase and group velocities. It is also worth to mention that the dispersion and number of surface branches are also dependent upon the period P that effects the interaction between neighboring wires. Finally, in our calculations, the resonant modes induced by the wires in the radiative frequency domain remain rather dispersionless, except when they interact with the sound line of the substrate folded back into the first Brillouin zone. Their frequencies are therefore rather similar to those obtained for a single ridge.

To end this section, we would like to mention that our methodology can also be applied to the problem of a periodic interface between two elastic isotropic materials or a line grating surface, and should also be useful for studying other excitations such as electromagnetic waves, or electronic states in the frame of an effective mass model.

This work has been made possible partly thanks to the Convention 991/4269 First-Europe ("Objectif 1") from the Walloonia Region of Belgium and the European Union.

Appendix

We use the following notation to give the expressions of A_n and B_n $\alpha = \frac{\omega P}{C_t^{(b)}}$, $\beta = \frac{C_t^{(b)} k}{\omega}$, $a_1 = \frac{9}{128}$, $a_2 = \frac{11\,025}{98\,304}$ and $b_1 = \frac{1}{8}$, $b_2 = \frac{225}{3\,072}$.

The summations which depend of the frequency ω and wavevector k are:

$$F_v = \sum_{n=n_0+1}^{\infty} \frac{\mathrm{e}^{\mathrm{i}n\alpha(1+\beta)}}{n^v}, \quad G_v = \sum_{n=n_0+1}^{\infty} \frac{\mathrm{e}^{\mathrm{i}n\alpha(1-\beta)}}{n^v}$$

where $v = 1/2,\ 3/2,\ 5/2,\ 9/2,\ 11/2$.

The expressions of A_n and B_n are:

$$A_1 = \frac{C_t^{(b)}}{\omega}\left[\left(\frac{5a_1}{2\alpha^2}F(7/2) - \frac{1}{2}F(3/2) - \frac{9a_2}{2\alpha^4}F(11/2)\right) + \mathrm{i}\left(\frac{3b_1}{2\alpha}F(5/2) - \frac{7b_2}{3\alpha^3}F(9/2)\right)\right]$$

$$A_2 = \frac{C_t^{(b)}}{\omega}\left[\left(\frac{3}{8}F(5/2) - \frac{35a_1}{8\alpha_2}F(9/2)\right) + \mathrm{i}\left(\frac{63b_2}{8\alpha^3}F(11/2) - \frac{15b_1}{8\alpha}F(7/2)\right)\right]$$

$$A_3 = \frac{C_t^{(b)}}{\omega}\left[\left(\frac{105a_1}{16\alpha^2}F(11/2) - \frac{5}{16}F(7/2)\right) + \mathrm{i}\left(\frac{35b_1}{8\alpha}F(9/2)\right)\right]$$

$$A_4 = \frac{C_t^{(b)}}{\omega}\left[\left(\frac{35}{128}F(9/2)\right) + \mathrm{i}\left(\frac{-315}{128\alpha}b_1F(11/2)\right)\right]$$

$$B_1 = \frac{C_t^{(b)}}{\omega}\left[\left(\frac{5a_1}{2\alpha^2}G(7/2) - 1/2G(3/2) - \frac{9a^2}{2\alpha^4}G(11/2)\right) + \mathrm{i}\left(\frac{3b_1}{2\alpha}G(5/2) - \frac{7b_2}{3\alpha^3}G(9/2)\right)\right]$$

$$B_2 = \frac{C_t^{(b)}}{\omega}\left[\left(\frac{3}{8}G(5/2) - \frac{35a_1}{8\alpha^2}G(9/2)\right) + \mathrm{i}\left(\frac{63b_2}{8\alpha^3}G(11/2) - \frac{15b_1}{8\alpha}G(7/2)\right)\right]$$

$$B_3 = \frac{C_t^{(b)}}{\omega}\left[\left(\frac{105}{16\alpha^2}a_1G(11/2) - \frac{5}{16}G(7/2)\right) + \mathrm{i}\left(\frac{35b_1}{8\alpha}G(9/2)\right)\right]$$

$$B_4 = \frac{C_t^{(b)}}{\omega}\left[\left(\frac{35}{128}G(9/2)\right) + \mathrm{i}\left(-\frac{315}{128\alpha}b_1G(11/2)\right)\right].$$

References

1. A.A. Maradudin, T. Michel, B. Djafari-Rouhani, A.R. Mc Gurn, A.R. Baghai-Wadji, in Continuum models and discrete systems, Vol. I, edited by G.A. Maugin (Longman, London, 1990).
2. V.P. Plessky, A.W Simonian, Phys. Lett. A **155**, 281 (1991).
3. B. Djafari-Rouhani, L. Dobrzynski, J. Phys. Cond. Matt. **5**, 8177 (1993).
4. B. Djafari-Rouhani, L. Dobrzynski, A. Khelif, Progr. Surf. Sci. **48**, 301 (1995).
5. A.A. Maradudin, in Recent developments in surface acoustic waves, edited by G.A. Maugin (Springer, Berlin, 1991).
6. B.A. Auld, J.J. Gagnepain, M. Tan, Electron. Lett. **12**, 650 (1976).
7. Yu.V. Gulyaev, V.P. Plessky, Zh. Tekh. Fiz. **48**, 447 (1978), Sov. Phys. Technical Physics **23**, 266 (1978).
8. N.E. Glass, A.A. Maradudin, Electron. Lett. **17**, 773 (1981).
9. A.R. Baghai-Wadji, A.A. Maradudin, Appl. Phys. Lett. **59**, 1841 (1991).
10. A.P. Mayer, W. Zierau, A.A. Maradudin, J. Appl. Phys. **69**, 1942 (1991).
11. A.N. Darinskii, J. Acoust. Soc. Am. **107**, 2447 (2000).
12. A.R. Baghai-Wadji, V.P. Plessky, A.V. Simonian, Soviet Physics Acoustics **38**, 442 (1992).
13. B. Djafari-Rouhani, A.A. Maradudin, J. Appl. Phys. **65**, 4245 (1989).
14. A.A. Maradudin, W. Zierau, Geophys. J. Int. **118**, 352 (1994).
15. V.P. Plessky, T. Thorvaldsson, IEEE Trans. Ultrason. **42**, 280 (1995).
16. A brief account of this work appeared in B. Djafari-Rouhani, A. Khelif, *the Proceedings of the 19th International Seminar on Surface Physics*, Vacuum **54**, 309 (1999).
17. A. Khelif, B. Djafari-Rouhani, J. Appl. Phys. **81**, 7141 (1997).
18. P.M. Morse, H. Feshbah, *Methods of theoretical physics* (Mc Graw-Hill, New York, 1953).
19. L. Dobrzynski, Surf. Sci. Rep. **6**, 119 (1986); *ibid.* **11**, 139 (1990).
20. J.E. Inglesfield, J. Phys. **L4**, 4 (1971).